

Spin and orbital order in the vanadium spinel MgV_2O_4

Elisa M. Wheeler,¹ Bella Lake,^{1,2} A. T. M. Nazmul Islam,¹ Manfred Reehuis,¹ Paul Steffens,³
Tatiana Guidi,⁴ and Adrian H. Hill⁵

¹*Helmholtz-Zentrum Berlin für Materialien und Energie, Hahn-Meitner-Platz 1, D-14109 Berlin, Germany*

²*Institut für Festkörperphysik, Technische Universität Berlin, Hardenbergstraße 36, D-10623 Berlin, Germany*

³*Institute Laue-Langevin, 6 rue Jules Horowitz, BP 156, 38042 Grenoble Cedex 9, France*

⁴*ISIS Facility, Rutherford Appleton Laboratory, Chilton, Didcot OX11 0QX, United Kingdom*

⁵*European Synchrotron Radiation Facility, 6 rue Jules Horowitz, BP 220, 38043 Grenoble Cedex 9, France*

(Received 22 September 2010; published 12 October 2010)

We present a study of the frustrated spinel MgV_2O_4 , which possesses highly coupled spin, lattice, and orbital degrees of freedom. Using large single crystal and powder samples, we find a distortion from spinel at room temperature (space group $F\bar{4}3m$) which allows for a greater trigonal distortion of the VO_6 octahedra and a low-temperature space group ($I\bar{4}m2$) that maintains the mirror plane symmetry. The magnetic structure that develops below 42 K consists of antiferromagnetic chains with a strongly reduced moment while inelastic neutron scattering reveals one-dimensional behavior and a single band of excitations. The implications of these results are discussed in terms of various orbital-ordering scenarios. We conclude that although spin-orbit coupling must be significant to maintain the mirror plane symmetry, the trigonal distortion is large enough to mix the $3d$ levels leading to a wave function of mixed real and complex orbitals.

DOI: [10.1103/PhysRevB.82.140406](https://doi.org/10.1103/PhysRevB.82.140406)

PACS number(s): 75.50.Ee, 71.70.Ej, 71.27.+a, 78.70.Nx

Geometrically frustrated magnets are characterized by competing interactions resulting in a highly degenerate low-energy manifold. In many cases the degeneracy is eventually lifted at low temperatures by a lattice distortion. In compounds where the magnetic ions also possess orbital degeneracy, orbital ordering can influence the exchange interactions and lift the frustration. The vanadium spinels AV_2O_4 , where A is diamagnetic Cd^{2+} , Zn^{2+} , or Mg^{2+} provide ideal systems to study the interactions between spin, lattice, and orbital degrees of freedom.¹ In these compounds the magnetic V^{3+} ions possess orbital degeneracy and form a frustrated pyrochlore lattice with direct exchange interactions between nearest neighbors providing a direct coupling to the orbital configuration. The interplay of orbital and spin physics has been studied in other systems like the perovskite vanadates (RVO_3 , R is a rare earth) which show a strong correlation between orbital ordering and magnetic structure.² However, in these compounds the couplings are unfrustrated and indirect, occurring via super exchange through oxygen. In contrast the magnetic structure and excitations in the spinel vanadates are more sensitive to orbital ordering and thus characteristic of it. Furthermore the additional component of frustration allows for the possibility of exotic ground states. Indeed the nature of the ground state in the spinel compounds has generated intense theoretical interest over the past eight years³⁻⁶ but has remained an unresolved experimental issue which we will address in this Rapid Communication.

The electronic configuration of V^{3+} is $3d^2$ leading to a single-ion spin $S=1$. Each V^{3+} ion is located at the center of edge sharing VO_6 octahedra which create a crystal field that splits the d orbitals and lowers the energy of the three t_{2g} orbitals by approximately 2.5 eV.⁷ These levels are usually assumed to be degenerate (ignoring the small trigonal distortion which will be discussed later) so that the two d electrons of V^{3+} randomly occupy the three t_{2g} orbitals, introducing an

orbital degree of freedom. These compounds undergoes a structural transition (T_S) from cubic to tetragonal which partially lifts the orbital degeneracy. A magnetic transition to long-range antiferromagnetic order occurs at a lower temperature (T_N). This Rapid Communication describes a comprehensive single-crystal investigation with supporting powder measurements of the crystal structure, magnetic structure, and magnetic excitations of MgV_2O_4 , which allows the orbital ordering to be determined and reveals the interplay between frustrated magnetism and orbital physics.

All measurements of the AV_2O_4 series have so far been performed on powder samples. ZnV_2O_4 is the most extensively studied member of the series. Powder neutron-diffraction measurements reveal a cubic to tetragonal structural phase transition at $T_S=51$ K, where the tetragonal c axis becomes suppressed and the space group is $I4_1/amd$.⁸ Long-range antiferromagnetic order occurs at $T_N=40$ K with an ordering wave vector of $\mathbf{k}=(0,0,1)$. Powder inelastic neutron scattering (INS) reveals a change in line shape of the magnetic fluctuations at T_S attributed to a change from three-dimensional to one-dimensional coupling.⁹ The tetragonal distortion at T_S causes the t_{2g} levels to split into a lower d_{xy} level and a twofold degenerate d_{yz}/d_{xz} level as shown in Fig. 1. One of the two d electrons occupies the d_{xy} level leading to antiferromagnetic chains in ab plane along the $[1,1,0]_{\text{cubic}}$ and $[1,\bar{1},0]_{\text{cubic}}$ directions. The second electron occupies either d_{yz} or d_{xz} or some combination and is responsible for the interchain coupling along $[1,0,1]_{\text{cubic}}$ and $[0,1,1]_{\text{cubic}}$. Models proposed for ZnV_2O_4 either place the second electron in a real combination of the d orbitals thus maintaining the orbital quenching or in a complex combination resulting in unquenched orbital moment. We will consider the three main models.

The first model is a real orbital ordered (ROO) model where the Kugel-Khomskii exchange Hamiltonian is introduced on the pyrochlore lattice. The ground state consists of

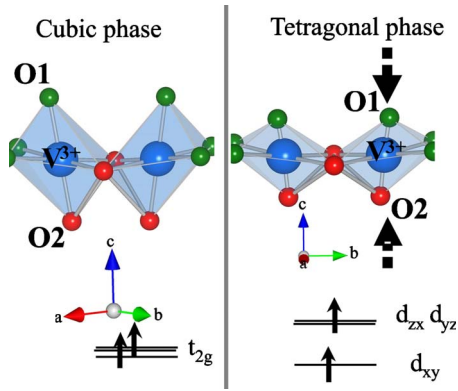


FIG. 1. (Color online) VO_6 octahedra along the chain direction in both the cubic and tetragonal phases (distortions have been exaggerated). The trigonal distortion slightly splits the t_{2g} levels in the cubic phase. In the tetragonal phase the oxygen octahedra are compressed causing large splitting of the t_{2g} levels.

alternating occupation of the d_{yz} or d_{xz} orbital in successive layers along the c axis.³ It gives rise to weak and frustrated ferromagnetic interchain coupling and no spin anisotropy. However, it implies that the space group is $I4_1/a$, which has lower symmetry than that of ZnV_2O_4 . Therefore a complex orbital ordering model (COO) was proposed that is compatible with the space group $I4_1/amd$ of ZnV_2O_4 , which has additional mirror and diamond glide planes. In this model the second electron occupies the orbital ($d_{yz} \pm id_{xz}$), which has unquenched orbital moment of $L=1$.⁴ The resulting interchain coupling is frustrated and antiferromagnetic and is expected to be larger than in the ROO case. It is favored when the spin-orbit coupling is strong in comparison to the interchain exchange interaction because the crystal can lower its energy by aligning L opposite to S . This scenario satisfies the spin-orbit interaction resulting in a reduced moment of $1 \mu_B$ compared to the spin only value of $2 \mu_B$ in ROO. In contrast the ROO model is favored when the interchain exchange interaction is dominant because it reduces the electron overlap and thus the energy of the frustrated bond. The third model considers the proximity of ZnV_2O_4 to the itinerant-electron boundary.⁶ Electron band-structure calculations imply a structural distortion where the vanadium-vanadium bond distances, $d(\text{V-V})$, alternate along the interchain directions. The shorter bond is predicted to be 2.92 \AA , below the limit for itinerancy. It is therefore described as a homopolar bond (HPB) characterized by partial electronic delocalization which results in ferromagnetic alignment of spins and release of interchain frustration. In this model the wave function would be the real combination of orbitals ($d_{yz} \pm d_{xz}$) with no net orbital moment.

Further distortions of the VO_6 octahedra besides the tetragonal distortion considered by these models are possible in the AV_2O_4 compounds. These could mix the d orbitals and completely remove their degeneracies resulting in a general wave function, e.g., $\alpha d_{xy} + \beta d_{xz} + \gamma d_{yz} + \epsilon(e_g)$. Indeed a trigonal distortion is already present in the cubic phase of ZnV_2O_4 . If the resulting splitting dominates over the exchange interaction or spin-orbit coupling then a wave function similar to that found for the related material MnV_2O_4

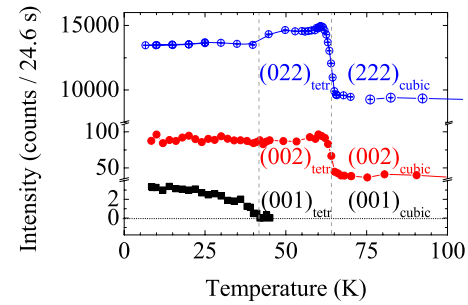


FIG. 2. (Color online) Neutron single-crystal diffraction results. Intensity of both the main Bragg reflections, (222), and the supercell reflections, (002), show a jump at T_S . At T_N , magnetic Bragg reflections at structural absences such as the (001) appear.

may result where α , β , γ , and ϵ are all nonzero and mostly real.¹⁰

The lack of large single crystals has prevented the full determination of the structural and magnetic behavior of the AV_2O_4 series. Here we report a single-crystal study of MgV_2O_4 . This material was investigated by Plumier and Tardieu¹¹ who observed magnetic order at low temperatures. Magnetic susceptibility, specific heat and powder x-ray diffraction measurements by Mamiya *et al.*¹² showed two transitions at $T_S=65 \text{ K}$ and $T_N=42 \text{ K}$ with the system changing from cubic to tetragonal below T_S . Here we describe x-ray and neutron diffraction and INS in the cubic, tetragonal, and magnetic phases. The data are used to distinguish between the theoretical pictures and is found to favor a mixture of real and complex orbitals with equal amplitudes of d_{xz} and d_{yz} .

To precisely determine the crystal and magnetic structure of MgV_2O_4 we carried out two complementary diffraction experiments. The four-circle diffractometer E5 at the BER II reactor (Helmholtz-Zentrum Berlin) was used with a wavelength $\lambda=0.89 \text{ \AA}$ along with a 3 mm Er filter and $\lambda=2.38 \text{ \AA}$ with a pyrolytic graphite filter to measure a large (187 mm^3) high-quality single-domain crystal.¹³ Powder x-ray measurements were made using the ID31 diffractometer at the European Synchrotron Radiation Facility with $\lambda=0.5 \text{ \AA}$ at 10 K and $\lambda=0.4 \text{ \AA}$ at 300 K. Refinements were performed using the FULLPROF (Ref. 14) and XTAL programs.¹⁵

First we consider the room-temperature results where the system has cubic symmetry. The single-crystal neutron diffraction revealed the presence of low intensity reflections of the type $(h00)$, where $h=2n$ and $(hk0)$, where $h,k=2n$, which are forbidden in the spinel, $Fd\bar{3}m$ (Fig. 2). They reveal the loss of the diamond glide plane and indicate that the space group is $F\bar{4}3m$. The trigonal point-group symmetry of the vanadium site characteristic of the spinel is maintained. Refinement of the room temperature x-ray and neutron diffraction yield the results listed in Table I. The vanadium ions were found to remain at the ideal spinel position. Only the oxygen distort the lattice from spinel to increase the trigonal distortion around the vanadium ion.

Low-temperature x-ray powder diffraction showed that at T_S no new Bragg reflections appear but that peaks split with an intensity ratio of 2:1 indicating a cubic to tetragonal structural phase transition where the c -lattice parameter is sup-

TABLE I. Lattice parameters and fractional coordinates in the tetragonal (6 K) and cubic (300 K) phases. In the cubic phase Mg sits at $4a(0,0,0)$ and $4c(\frac{1}{4}, \frac{1}{4}, \frac{1}{4})$. Both O and the V sites are $16e(x,x,x)$. In the tetragonal phase Mg sits at $2a(0,0,0)$ and $2d(0, \frac{1}{2}, \frac{3}{4})$ while the O and V sites are $8i(x,0,z)$.

	6 K $I\bar{4}m2$		300 K $F\bar{4}3m$
	$a=5.96047(3) \text{ \AA}$		$a=8.42022(1) \text{ \AA}$
	$c=8.37927(5) \text{ \AA}$		
	$V=297.693(3) \text{ \AA}^3$		$V=596.995(2) \text{ \AA}^3$
$x(\text{O1})$	0.7648(2)	$x(\text{O1})$	0.38623(10)
$z(\text{O1})$	0.3872(2)		
$x(\text{O2})$	0.7743(2)	$x(\text{O2})$	0.86623(9)
$z(\text{O2})$	0.8661(2)		
$x(\text{V})$	0.250(2)	$x(\text{V})$	0.6251(2)
$z(\text{V})$	0.625(1)		

pressed $c/a=0.9941(1)$. This value is in good agreement with $c/a=0.993$ found previously.¹² For the single-crystal neutron diffraction we ensured a single tetragonal domain by applying a uniaxial pressure of approximately 0.5 MPa along [001]. Figure 2 shows a jump in the intensity of Bragg reflections at $T_S=64$ K due to a change in extinction parameters. The low-temperature data set matched the space group $I\bar{4}m2$. This space group is characterized by a mirror plane and twofold rotational axis which ensures that the spatial wave functions of the electrons consists of equal amplitudes of d_{xz} and d_{yz} , a combination favored by spin-orbit coupling and trigonal distortion. Again we found the vanadium was not displaced from ideal spinel position. Therefore $d(\text{V-V})$ is not significantly affected by the tetragonal distortion. Within the tetragonal plane there are two inequivalent intrachain bonds both of distance $d(\text{V-V})=2.9802 \text{ \AA}$ while between the planes there are four interchain bonds of $d(\text{V-V})=2.9714 \text{ \AA}$. This result discounts the HPB model for MgV_2O_4 , which is characterized by alternating bond lengths, the smaller of which should be less than the limit for itinerancy of 2.94 \AA .

New Bragg reflections appear in the neutron diffraction below $T_N=42$ K and can be indexed with the ordering wave vector $\mathbf{k}=(0,0,1)$ indicating an antiferromagnetic spin alignment along the chains as found previously.¹¹ The spins point predominantly along the c axis with a moment of $\mu_z=0.47(1) \mu_B$. A tilt of $8(1)^\circ$ from the c axis, similar to the tilt of the oxygen octahedra along the chains, was identified by a finite intensity on the (001) reflection [Fig. 3(a)]. The moment is greatly reduced from the $2 \mu_B$ expected for ROO in the case of full magnetic ordering and even reduced from the $1 \mu_B$ expected for COO. It is smaller than in CdV_2O_4 or ZnV_2O_4 , which have moments of $1.19 \mu_B$ and $0.63 \mu_B$, respectively.

We made INS measurements on the IN20 spectrometer with the Flatcone detector at the Institute Laue-Langevin using the detwinned crystal at 2 K with the tetragonal plane in the horizontal scattering plane. We used a Si monochromator and analyzer with a fixed final wave vector $k_f=3 \text{ \AA}^{-1}$ ($E_f=18.6 \text{ meV}$). At low energies we observe intense scattering along two sets of stripes in the tetragonal plane which are perpendicular to each other [Fig. 3(b)]. At higher energy these stripes split into two branches. The stripes indicate that the modes disperse strongly along the straight weakly coupled chains of antiferromagnetic spins confirming occupation of the d_{xy} orbital. Further measurements at the MERLIN time-of-flight spectrometer at ISIS using a powder sample and incident energy of 200 meV reveal a single band of excitations extending up to 65 meV. No magnetic scattering was observed between 65 meV and 110 meV as shown in Fig. 3(c).

The magnetic excitation spectrum has been calculated by Perkins and Sikora⁵ for both the COO and ROO. In the COO there are acoustic and optic bands. The optic band is predicted to have comparable scattering weight to the acoustic band and is a direct consequence of unquenched orbital moment. It is expected to lie at a higher energy, well separated from the acoustic band due to the spin-orbit coupling. For the ROO model gapless acoustic spin-wave modes are predicted which disperse up to 40 meV along the chain but are only weakly dispersive between chains. The magnetic excitation spectrum of MgV_2O_4 appears to be in better agreement with

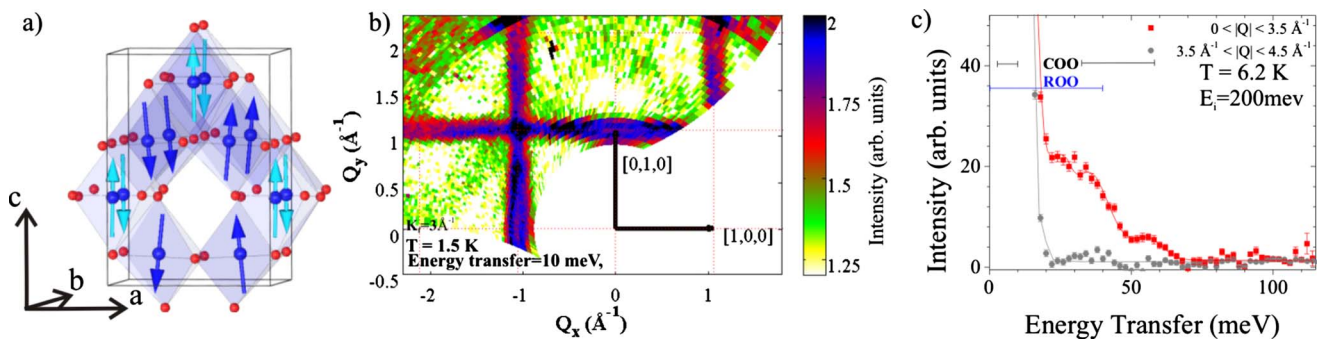


FIG. 3. (Color online) (a) The tetragonal unit cell with only vanadium (blue/black) and oxygen (red/gray) ions shown. Light/dark blue (gray/black) arrows indicate the magnetic-moment directions of the two perpendicular antiferromagnetic chains. (b) Single crystal INS data measured at 10 meV and 1.5 K labeled in tetragonal notation. The intense stripes indicate highly one-dimensional perpendicular chains of spins. (c) Background subtracted INS data from a powder sample summed over two $|Q|$ ranges. Magnetic signal appears in the low $|Q|$ range while at higher $|Q|$ magnetic intensity is suppressed due to the magnetic form factor of the V^{3+} ion. No magnetic scattering is observed above 65 meV. Lines indicate the bandwidths predicted for the COO model and ROO model (Ref. 5).

the ROO model. We do indeed observe highly dispersive excitations contrary to expectations for largely local-orbital excitations in the COO model.

These results have implications for the orbital and magnetic behavior of MgV_2O_4 , which we now discuss. The HPB model is discounted since we have no alternation of the interchain $d(\text{V-V})$. The COO model has unquenched orbital angular momentum that reduces the total magnetic moment.⁴ We do indeed observe a strongly reduced ordered moment which is even smaller than the $1 \mu_B$ expected. The 8° tilt of the moment implies some anisotropy indicating the presence of spin-orbit coupling. However, the measured magnetic excitations are not consistent with a large unquenched orbital moment but are in better agreement with the ROO model. Here the orbital moment is quenched and the total moment should be $2 \mu_B$, however, it can be strongly reduced due to quantum fluctuations known to suppress ordering in one-dimensional systems with small and frustrated interchain coupling.^{3,16} ROO was the original model proposed for AV_2O_4 systems. It was discounted as a description of ZnV_2O_4 because the mirror plane perpendicular to the tetragonal a - or b -axis constrains the occupation of the d_{yz} and d_{xz} orbitals to be equivalent on every site. This constraint also holds for MgV_2O_4 . Together the experimental evidence suggests that the orbital wave function of the V^{3+} ions in MgV_2O_4 is neither purely real nor complex but is instead a mixture of the two.

To compare MgV_2O_4 to other AV_2O_4 compounds consider the general wave function $\alpha d_{xy} + \beta d_{xz} + \gamma e^{i\phi} d_{yz}$. When the tetragonal distortion is much larger than the trigonal distortion, which would split and mix the t_{2g} orbitals, we expect

$\alpha \sim 1$, $\beta, \gamma \ll 1$ for the first electron and $\alpha \ll 1$, $\beta, \gamma \sim 1/\sqrt{2}$ for the second electron. In the case of ZnV_2O_4 , density function theory calculations within the $I4_1/amd$ space group show the trigonal distortion is small and spin-orbit coupling dominates giving rise to COO (i.e., $\phi = \pi/2$, $\beta = \gamma = 1/\sqrt{2}$ for the second electron).¹⁷ In contrast for MnV_2O_4 , where the space group is $I4_1/a$ and both the diamond glide plane and mirror plane are lost, the trigonal distortion is large. As a result both electrons occupy a mostly real mixture of d orbitals, $\phi \approx 0$ and $\beta \neq \gamma$.¹⁰ The influence of spin-orbit coupling is weak in comparison and the orbital moment is small at $0.34 \mu_B$.^{10,18} We suggest that the wave function of MgV_2O_4 sits between these two examples. The influence of the spin-orbit coupling is substantial because the mirror plane is maintained constraining $\beta = \gamma$. Nevertheless the large excitation bandwidth indicates that the orbital moment is not maximal, i.e., $\beta < 1/\sqrt{2}$ and $\phi \neq \pi/2$ for the second electron, suggesting that the trigonal distortion also plays a significant role. On the other hand, the interchain exchange energy which would be minimized by unequal occupation of d_{xz} and d_{yz} is too weak to influence the orbital wave function.

In summary, we propose that while the tetragonal distortion is dominant, the smaller spin-orbit coupling and trigonal distortion are of similar strengths and the exchange energy is weak. These results imply that the $3d$ electrons in MgV_2O_4 occupy a mixture of real and complex orbitals.

We thank N.B. Perkins, G.-W. Chern, M. Enderle, M. Tovar, A. Daoud-Aladine, and O. Tchernyshyov for useful discussions and D.N. Argyriou for use of Crystal Laboratory.

¹P. G. Radaelli, *New J. Phys.* **7**, 53 (2005).

²G. Khaliullin, *Prog. Theor. Phys. Suppl.* **160**, 155 (2005).

³H. Tsunetsugu and Y. Motome, *Phys. Rev. B* **68**, 060405 (2003).

⁴O. Tchernyshyov, *Phys. Rev. Lett.* **93**, 157206 (2004).

⁵N. B. Perkins and O. Sikora, *Phys. Rev. B* **76**, 214434 (2007).

⁶V. Pardo, S. Blanco-Canosa, F. Rivadulla, D. I. Khomskii, D. Baldomir, Hua Wu, and J. Rivas, *Phys. Rev. Lett.* **101**, 256403 (2008).

⁷J. Matsuno, A. Fujimori, and L. F. Mattheiss, *Phys. Rev. B* **60**, 1607 (1999).

⁸M. Reehuis, A. Krimmel, N. Büttgen, A. Loidl, and A. Prokofiev, *Eur. Phys. J. B* **35**, 311 (2003).

⁹S.-H. Lee, D. Louca, H. Ueda, S. Park, T. J. Sato, M. Isobe, Y. Ueda, S. Rosenkranz, P. Zschack, J. Íñiguez, Y. Qiu, and R. Osborn, *Phys. Rev. Lett.* **93**, 156407 (2004).

¹⁰S. Sarkar, T. Maitra, R. Valentí, and T. Saha-Dasgupta, *Phys. Rev. Lett.* **102**, 216405 (2009).

¹¹R. Plumier and A. Tardieu, *C. R. Hebd. Seances Acad. Sci.* **257**, 3858 (1963).

¹²H. Mamiya, M. Onoda, T. Furubayashi, J. Tang, and I. Nakatani, *J. Appl. Phys.* **81**, 5289 (1997).

¹³A. T. M. N. Islam, E. M. Wheeler, B. Lake, M. Reehuis, K. Siemensmeyer, K. Kiefer, and M. Tovar (unpublished).

¹⁴J. Rodríguez-Carvajal, *Physica B* **192**, 55 (1993).

¹⁵S. R. Hall, D. J. du Boulay, and R. Olthof-Hazekamp, *Xtal3.7 System* (University of Western Australia, Perth, Australia, 2000).

¹⁶Y. Motome and H. Tsunetsugu, *Phys. Rev. B* **70**, 184427 (2004).

¹⁷T. Maitra and R. Valentí, *Phys. Lett. B* **99**, 126401 (2007).

¹⁸G.-W. Chern, N. Perkins, and Z. Hao, *Phys. Rev. B* **81**, 125127 (2010).